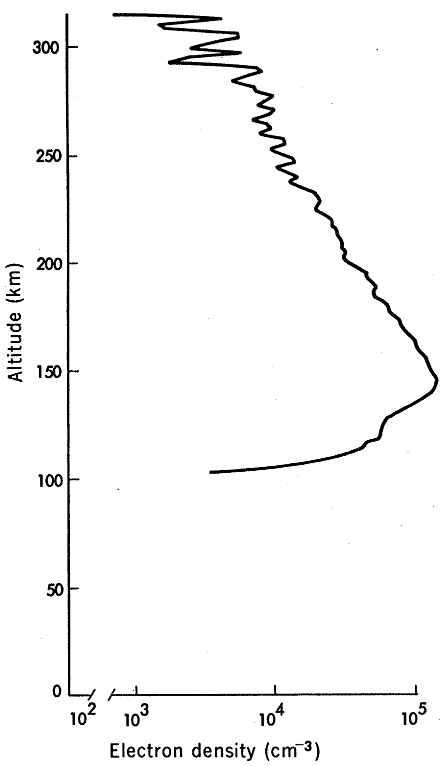

Fig. 7. Electron density in the ionosphere of Mars versus altitude. This measurement was made on the day side of Mars during revolution 2.

measurements to be remarkably reproducible from one pass to the next. For example, values obtained for the peak electron density and the topside scale height differ by less than 5 percent. The altitude of the ionization peak changes somewhat from one pass to another, but this effect is due partially to elevation differences on the surface.

The results reported here show that the density and temperature of the Martian ionosphere have been reduced since 1969 (*4*), but that they are higher than during the quiet solar conditions prevailing at the time of the Mariner 4 mission in 1965. However, the most notable difference between measurements from Mariner 9 and those from earlier spacecraft is the increased altitude of the ionization peak, which shows that the atmospheric region below 145 km is warmer than before. This observation is consistent with the measured temperatures in the lower atmosphere.

A. J. KLIORE, D. L. CAIN
G. FJELDBO, B. L. SEIDEL
Jet Propulsion Laboratory, California Institute of Technology, Pasadena 91103

S. I. RASOOL
National Aeronautics and Space Administration, Washington, D.C.

References and Notes

1. A. J. Kliore, D. L. Cain, G. S. Levy, in *Space Research VI* (North-Holland, Amsterdam, 1967), p. 226.
2. G. Fjeldbo and V. R. Eshleman, *Planet. Space Sci.* **16**, 1035 (1968).
3. A. J. Kliore, G. Fjeldbo, B. L. Seidel, in *Space Research XI* (Akademie-Verlag, Berlin, 1971), p. 165.
4. G. Fjeldbo, A. J. Kliore, B. L. Seidel, *Radio Sci.* **5**, 381 (1970).
5. A. J. Kliore, *Proceedings of the Workshop on the Mathematics of Profile Inversion* (Ames Research Center, Moffett Field, Calif., in press).
6. P. Gierasch and R. Goody, *Planet. Space Sci.* **16**, 615 (1968).
7. A. E. E. Rogers, M. E. Ash, C. C. Counselman, I. I. Shapiro, G. H Pettengill, *Radio Sci.* **5**, 465 (1970); R. M. Goldstein, W. G. Melbourne, G. A. Morris, G. S. Downs, D. A. O'Handley, *ibid.*, p. 475; G. H. Pettengill, A. E. E. Rogers, I. I. Shapiro, *Science* **174**, 1321 (1971).
8. A. Kliore, *Bull. Amer. Astron. Soc.* **2**, 202 (1970).
9. C. A. Barth and C. W. Hord, *Science* **173**, 197 (1971); C. W. Hord, *Icarus*, in press.
10. C. Sagan, J. Veverka, P. Gierasch, *Icarus* **15**, 253 (1971).
11. K. C. Herr, D. Horn, J. M. McAffee, G. C. Pimentel, *Astron. J.* **75**, 833 (1970).
12. We thank the personnel of the Mariner 1971 Project and the Deep Space Network at the Jet Propulsion Laboratory who have delivered our data with their usual competence. We thank M. J. Sykes for his essential contribution to data analysis and J. W. Zielenbach for supplying us with excellent navigation data. This report presents the results of one phase of research carried out at the Jet Propulsion Laboratory, California Institute of Technology, under NASA contract NAS-7-100.

27 December 1971

Mariner 9 Celestial Mechanics Experiment: Gravity Field and Pole Direction of Mars

Abstract. *Analysis of the Mariner 9 radio-tracking data shows that the Martian gravity field is rougher than that of Earth or the moon, and that the accepted direction of Mars's rotation axis is in error by about 0.5°. The new value for the pole direction for the epoch 1971.9, referred to the mean equatorial system of 1950.0, is right ascension* $\alpha = 317.3° \pm 0.3°$, *declination* $\delta = 52.6° \pm 0.2°$. *The values found for the coefficients of the low-order harmonics of Mars's gravity field are as follows:* $J_2 = (1.96 \pm 0.01) \times 10^{-3}$, *referred to an equatorial radius of 3394 kilometers;* $C_{22} = -(5 \pm 1) \times 10^{-5}$; *and* $S_{22} = (3 \pm 1) \times 10^{-5}$. *The value for* J_2 *is in excellent agreement with the result from Wilkins' analysis of the observations of Phobos. The other two coefficients imply a value of* $(2.5 \pm 0.5) \times 10^{-4}$ *for the fractional difference in the principal equatorial moments of inertia; the axis of the minimum moment passes near 105°W.*

The preliminary results on the gravity field of Mars and the direction of its spin axis obtained from the Mariner 9 radio-tracking data provide the basis for this report. These data consist primarily of counted Doppler data (changes in the round-trip phase delay of the radio signal), converted to values averaged over 1-minute count times (*1*). The observations span two periods (*2*): (i) from orbit insertion on 14 November to orbit trim on 16 Novem-

Table 1. Characteristics of the Mariner 9 orbit.

Parameter	Before trim	After trim
Epoch (U.T.)	14 Nov., 00:42	16 Nov., 02:58
Semimajor axis (km)	13,046	12,636
Eccentricity	0.63282	0.62173
Inclination to Martian equator (deg)	64.35	64.37
Latitude of periapsis (deg)	—22.7	—22.1
West longitude of initial periapsis (deg)	102.3	117.2
Periapsis altitude (km)	1397	1387
Anomalistic orbital period (hours)	12.567	11.980

Table 2. Direction of the pole of Mars. Pole is given for epoch 1971.9 and referred to the mean equinox and equator of 1950.0.

Angle	Nominal value (*6*)	Orbit phase radio-tracking data	Far-encounter TV pictures of landmarks	Far-encounter TV pictures of Martian satellites
Right ascension, α (deg)	316.9	317.3 ± 0.3	317.5 ± 0.9	317.2 ± 0.5
Declination, δ (deg)	53.0	52.6 ± 0.2	52.9 ± 0.9	52.9 ± 0.3

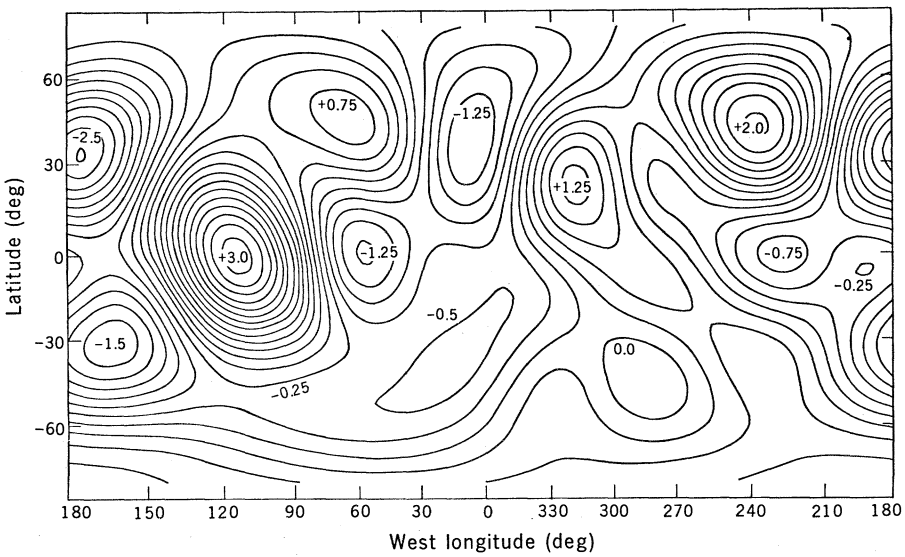

Fig. 1. Contours of equivalent surface heights deduced from a sixth-degree solution for the Martian gravity field. These contours represent the deviations from sphericity of a uniformly dense body with external potential given by the first sixth-degree solution, with the effect of J_2 omitted. Contours are labeled in kilometers; the contour interval is 250 m.

ber 1971 and (ii) from 16 November to 3 December 1971. The first period consists of almost four complete revolutions; the second consists of 33. The characteristics of the orbit before and after the trim are given in Table 1.

The Doppler data are affected noticeably by the inhomogeneities in Mars's gravity field and thus by its rotation vector. In order to estimate the parameters associated with these characteristics, we compared the data with precise theoretical computations based on double-precision numerical integration of the equations of motion of the spacecraft with respect to Mars. These equations included the perturbing accelerations due to the gravity field of Mars, the sun, and planets, direct sunlight pressure, and gas leakages. The Earth-Mars orbit was fixed in accord with determinations based on radar data of the inner planets (*3*). Tracking station locations were based on determinations from past Mariner missions with the rotational motions of Earth modeled in the standard manner. To account for the effects of the propagation medium, semiempirical models of the atmosphere and ionosphere were used. The relevant variational equations were integrated numerically in double precision; the parameters estimated in our first solution were as follows: the six initial conditions, or state vector, for the spacecraft's orbit; 35 coefficients in the gravity model; and the right ascension, α, and declination, δ, of Mars's rotation axis. The gravity-field potential was represented by a spherical harmonic expansion:

$$U = -\frac{GM_{\text{♂}}}{r}\left[1 - \sum_{n=2}^{\infty} J_n \left(\frac{R}{r}\right)^n P_{n0}(\sin\theta) + \sum_{n=2}^{\infty}\sum_{m=1}^{n}\left(\frac{R}{r}\right)^n P_{nm}(\sin\theta)\,(C_{nm}\cos m\lambda + S_{nm}\sin m\lambda)\right]$$

where G is the constant of gravitation; $M_{\text{♂}}$ is the mass of Mars, fixed at the value obtained from the Mariner 4 flyby (*4*); R is the equatorial radius of Mars, taken as 3394 km; r is the radial distance of the orbiter from Mars; and P_{nm} denotes the associated Legendre polynominals, with θ the latitude and λ the longitude on Mars. All coefficients through the fifth degree plus the even-order sixth degree were included for this solution except for S_{21} and C_{21}, which were omitted because of the presence of the pole angles α and δ as parameters (*5*). The result for the pole position is given in Table 2 and is compared with the accepted value based on optical observations from Earth (*6*). Also listed are two other determinations based on pictures taken by the Mariner television camera. The first of these (from S. N. Mohan), obtained by tracking features on the surface of Mars from a series of far-en-

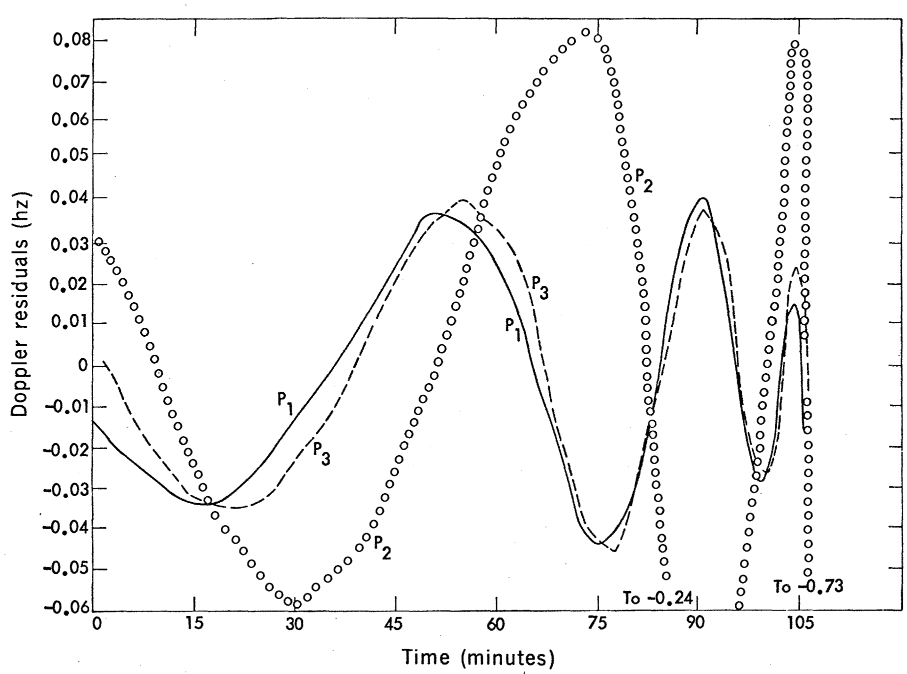

Fig. 2. Residuals from short-arc fits near the first three periapsis passages of Mariner 9. Only the state vector was estimated; the residuals represent the effects of the Martian gravity field. The results for the first and third passages, P_1 and P_3, are similar because the orbital period was almost half the spin period of Mars (see Table 1). For the radio frequency of about 2300 Mhz, 1 mm/sec $\simeq$ 0.015 hz. Near periapsis passage, which occurred at about t = 102 minutes, the speed of the Mariner 9 spacecraft was about 4 km/sec. Earth occultation precluded extension of the data past periapsis.

Table 3. Coefficients for the second-degree harmonics of the gravity field referred to a radius of 3394 km.

Coefficient	Nominal value (*8*)	Mariner 9 value	Moon (*14*)		Earth (*15*)	
			Unscaled	Scaled to Mars (*9*)	Unscaled	Scaled to Mars (*9*)
J_2	$(1.968 \pm 0.006) \times 10^{-3}$	$(1.96 \pm 0.01) \times 10^{-3}$	$(0.200 \pm 0.002) \times 10^{-3}$		1.083×10^{-3}	
C_{21}	0	$< 3 \times 10^{-6}$				
S_{21}	0	$< 3 \times 10^{-6}$				
C_{22}	*	$-(5 \pm 1) \times 10^{-5}$	$(2.4 \pm 0.5) \times 10^{-5}$	0.5×10^{-5}	0.16×10^{-5}	1.0×10^{-5}
S_{22}	*	$(3 \pm 1) \times 10^{-5}$	$(0.5 \pm 0.6) \times 10^{-5}$	0.1×10^{-5}	-0.09×10^{-5}	-0.6×10^{-5}

* No value available before the Mariner 9 mission.

counter pictures, is in agreement with the accepted value and is of comparable accuracy. The second determination (from T. C. Duxbury), based on pictures of Phobos and Deimos and on the assumption that the orbital inclinations of these satellites to the Martian equator were known to within 0.2°, also gives a result for the pole direction consistent with both the nominal value and that deduced from the radio-tracking data, but has an uncertainty of about 0.5° in both coordinates. To test the significance of the pole direction correction implied by the radio data, several solutions were carried out from disjoint data sets with the pole direction alternately fixed at the radio and optical values and with S_{21} and C_{21} added to the parameter set. In all cases, the "radio" pole yielded substantially smaller values for S_{21} and C_{21}, a result which tends to support the radio value. Ultimately, the Mariner 9 mission should yield a pole direction with an uncertainty no greater than about 0.1°.

Of greater direct scientific interest is the solution for the gravity field itself. In view of the Mariner 9 periapsis altitude, which corresponds to about 1/15 of the circumference of Mars, the tracking data will yield some information on harmonics up to the 15th degree and order. However, a meaningful, complete solution of this extent will probably not be obtained from Mariner 9; its large orbital eccentricity, near-critical inclination (*7*), and near-resonant period imply that only for a small portion of the planet near the periapsis latitude of —22° will the tracking data be sensitive to gravity anomalies of this order. Furthermore, the estimates of the coefficients of the terms of intermediate degree and order will be highly correlated with one another. For the limited span of observations presently available, solutions for the individual terms are considered reliable only through the second degree; these are shown in Table 3. The uncertainties given are based on the above facts and on comparisons of results from three almost complete sixth-degree solutions that utilized disjoint data sets bounded by periapsis passages. The first contained data from orbital revolutions 4 to 10, the second from revolutions 19 to 25, and the third from revolutions 31 to 37. The value for J_2 is in excellent agreement with Wilkins' value, which was based primarily on Earth-based telescopic observations of Phobos between 1877 and 1928 (*8*). The values for C_{22} and S_{22} imply that fractional difference, $(\mathrm{B} - \mathrm{A})/\mathrm{M}_{♂} R^2$, in the equatorial principal moments of inertia is $(2.5 \pm 0.5) \times 10^{-4}$ and that the axis of the minimum moment of inertia passes approximately through 105°W.

Although the other individual terms for the sixth-degree solutions are not too meaningful, the ensemble is perhaps more reliable. The contours of constant equivalent surface heights are similar for the three solutions; the contours for the first solution, omitting the effect of J_2, are shown in Fig. 1. The deviations from a spheroid are seen to vary from about − 2.5 to + 3 km. These variations imply substantial stresses and, if confirmed by further analysis, will establish Mars as gravitationally much "rougher" than either Earth or the moon. Scaling the variations with the square of the

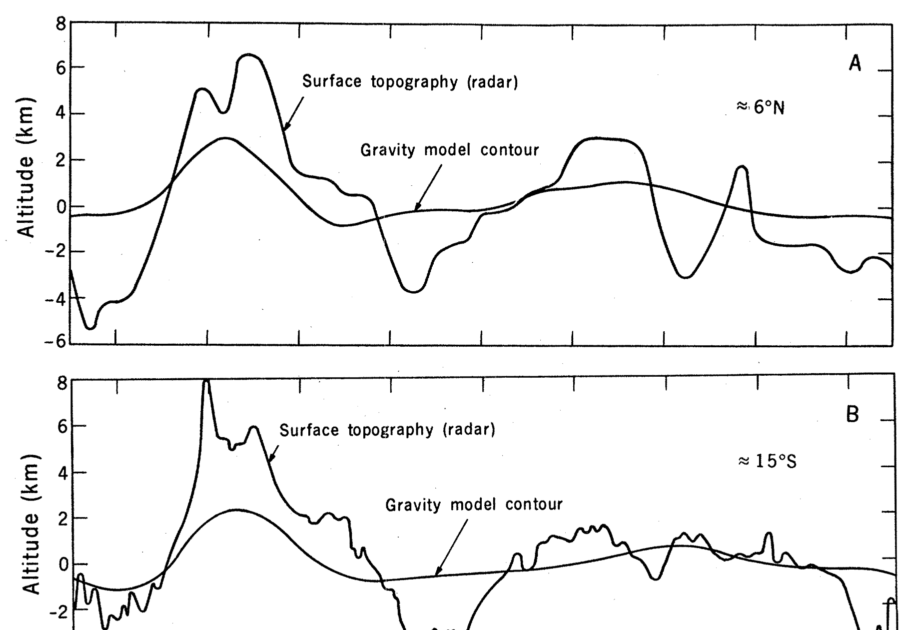

Fig. 3. Comparison of surface contours deduced from sixth-degree gravity model (see Fig. 1) with radar measurements (*10*) of surface-height variations near the Martian equator. The 1971 radar data (B) are of substantially higher resolution than the 1969 data (A).

surface acceleration of gravity (*9*), we obtain the comparative results shown in Table 3 for the three bodies for equivalent surface resolution.

The gravity solutions were limited to data covering six orbital revolutions and thus do not extract all of the gravity information inherent in the complete set of observations. This assertion is supported by the results from predictions which exhibit gradually increasing residuals to about 10 hz after several revolutions. The post-fit residuals for the data used in the solutions nowhere exceed about 0.05 hz, as compared with the observed noise level of 0.005 hz. With more data, the gravity solution, at least near the periapsis latitude, will be of finer resolution. Even with the present limited data set, short-arc fits covering the periapsis region can be used for local determinations. Residuals obtained from several short-arc solutions near periapsis in which only the spacecraft state vector was estimated are displayed in Fig. 2. Consistency between solutions for arcs with almost the same periapsis point on the Martian surface is evident, as is the disparity for periapsis corresponding to positions on opposite sides of Mars. Analysis of these residuals to estimate the high-frequency gravity variations, which may possibly reveal the presence of mascons, has not been completed. Later in the mission, when the orbit geometry improves and Earth occultations end, the data will be much more favorable for this type of analysis.

A comparison of the gravity contours exhibited in Fig. 1 with surface heights determined from Earth-based radar observations (*10*) is instructive. The radar data are confined to the equatorial region ($\pm 20°$ in latitude); therefore, we show in Fig. 3 surface heights for two representative latitudes as compared with the corresponding gravity-potential contours. The low-frequency components of the surface-height variations correlate well with those of the gravity-potential contours. In particular, the gravity contours peak within about 20° of the surface-height maxima. In some places the amplitudes of the variations in surface heights are severalfold larger than those in the gravity contours. Such disparities are probably attributable to the averaging effect of the low-resolution gravity model and to isostatic compensation. A quantitative apportionment must await the development of a better gravity model.

Measurements of surface pressure from other experiments (*11*), when combined with the gravity contours, also can be used to infer surface-height variations. Comparisons with the radar determinations, where they exist, will then allow important closure tests to be made. Only low-frequency components of the topography can be inferred because of the restricted surface resolution of the gravity data.

No useful upper bound on the density of the Martian exosphere at the periapsis altitude has been obtained as yet. This density affects the Doppler tracking data through the drag on the spacecraft, which in turn manifests itself most sensitively through secular changes in the orbital mean anomaly. The gravity-field variations, which also affect the mean anomaly, are periodic, thus affording a method of separation. Several rotations of Mars with respect to the spacecraft's position at periapsis probably are required for separation. Each such rotation takes about 20 days. The analysis presented here allows us to conclude only that the air density at periapsis is no greater than about 10^{-15} g/cm^3; most likely, it is far less.

In addition to Doppler observations, ranging or group-delay measurements have been made regularly since orbit insertion. These latter data will be used to test the predicted general relativistic effect of solar gravity on the round-trip delays (*12*) and, concomitantly, to improve the determination of the orbits of Earth and Mars. The data now extend over too small an arc to permit any scientific conclusions to be drawn. Continuation well past the superior conjunction of September 1972 is required for an accurate relativity test. Corresponding improvements in the orbits of Earth and Mars will then be sufficient to allow radar echo-delay data to be interpreted directly in terms of surface heights. Substantial improvements will also be possible in the interpretations of the Earth-Mercury and Earth-Venus radar observations.

J. LORELL, G. H. BORN
E. J. CHRISTENSEN
J. F. JORDAN, P. A. LAING
W. L. MARTIN, W. L. SJOGREN
Jet Propulsion Laboratory, California Institute of Technology, Pasadena 91103

I. I. SHAPIRO
R. D. REASENBERG, G. L. SLATER
Department of Earth and Planetary Sciences, Massachusetts Institute of Technology, Cambridge 02139

References and Notes

1. These data were obtained primarily at deep space stations at Goldstone, California (stations 12 and 14); Madrid, Spain (station 62); and Woomera, Australia (station 41). Apoapsis data were compressed to values averaged over 10 minutes.
2. Tracking data obtained prior to orbit insertion also have been analyzed. In particular, S. K. Wong and S. J. Reinbold have processed a 3-month arc obtaining one of the best determinations to date of the Earth-moon mass ratio. This new value is 81.3007 ± 0.0003, consistent with results from previous spacecraft (*13*); the uncertainty is due primarily to that of Earth-moon distance.
3. Effects on the Doppler data due to drifts in these ephemerides were estimated to be no more than a few millihertz during the month after the orbit insertion of Mariner 9.
4. This value (3,098,708 ± 9 in units of inverse solar masses) was determined by G. W. Null [*Bull. Amer. Astron. Soc.* **1**, 356 (1969)].
5. We assume that the rotation axis coincides with the principal axis of the maximum moment of inertia, which in turn defines our body-fixed Z-coordinate axis. If the direction of this axis in our inertial frame is known precisely, then estimates of C_{21} and S_{21} should tend to zero, because these coefficients will be proportional to off-diagonal terms of the moment of inertia tensor which vanish identically in this coordinate system. If the pole direction were not estimated and if it were in error, then nonzero values would in general be obtained for C_{21} and S_{21}. For a quantitative assessment, see J. Lorell, *J. Astronaut. Sci.*, in press.
6. G. de Vaucouleurs, *Icarus* **3**, 236 (1964).
7. At an inclination of about 63° (where $\cos^2 \theta = 0.2$), the first-order, long-period motion of periapsis due to J_2 vanishes.
8. G. Wilkins, in *Mantles of the Earth and Terrestrial Planets*, S. Runcorn, Ed. (Interscience, London, 1967), p. 77.
9. This scaling law follows from the assumption that gravity anomalies are equivalent if corresponding surface mass anomalies produce equal stresses. See, for example, W. M. Kaula, in *Trajectories of Artificial Celestial Bodies*, J. Kovalevsky, Ed. (Springer-Verlag, Berlin, 1966), p. 247.
10. G. H. Pettengill, C. C. Counselman, L. P. Rainville, I. I. Shapiro, *Astron. J.* **74**, 461 (1969); A. E. E. Rogers, M. E. Ash, C. C. Counselman, I. I. Shapiro, G. H. Pettengill, *Radio Sci.* **5**, 465 (1970); R. M. Goldstein, W. G. Melbourne, G. A. Morris, G. S. Downs, D. A. O'Handley, *ibid.*, p. 475; G. H. Pettengill, A. E. E. Rogers, I. I. Shapiro, *Science* **174**, 1321 (1971); G. S. Downs, R. M. Goldstein, R. R. Green, G. A. Morris, *ibid.*, p. 1324.
11. See results from ultraviolet spectroscopy, infrared spectroscopy, and S-band occultation experiments on Mariner 9 in this issue of *Science*; S-band occultation data also determine the radius of Mars at the point of occultation and can therefore be used to deduce gravity-field variations independently.
12. See, for example, J. D. Anderson, P. B. Esposito, W. L. Martin, D. O. Muhleman [*Jet Propulsion Lab. Tech. Mem. 33–499* (1971), p. 111] and I. I. Shapiro, M. E. Ash, R. P. Ingalls, W. B. Smith, D. B. Campbell, R. B. Dyce, R. F. Jurgens, G. H. Pettengill [*Phys. Rev. Lett.* **26**, 1132 (1971)].
13. J. D. Anderson, L. Efron, S. K. Wong, *Science* **167**, 277 (1970).
14. Moon gravity models, as obtained from Lunar Orbiter data, are still subject to large uncertainty; see J. Lorell, *Moon* **1**, 190 (1970). Perhaps the best model is that obtained by A. S. Liu and P. A. Laing [*Science* **173**, 1017 (1971)], whose values are used in Table 3.
15. E. M. Gaposchkin and K. Lambek, *J. Geophys. Res.* **76**, 4855 (1971).
16. We thank D. L. Cain, R. M. Georgevic, A. S. Liu, H. N. Royden, G. Sherman, S. Synnott, and the Mariner 9 navigation team, especially J. W. Zielenbach and D. H. Boggs, for their important contributions. We also thank T. C. Duxbury, S. N. Mohan, S. K. Wong, and S. J. Reinbold for permitting us to quote their results prior to publication.

27 December 1971